ISBN: 978-3-95450-261-5 ISSN: 2673-7000 doi: 10.18429/JACoW-NAPAC2025-MOP055

# LOW-CHARGE, HIGH-RESOLUTION BEAMLINE PREPARATION FOR THE NANOPATTERNED MICROBUNCHING EXPERIMENT AT ARGONNE WAKEFIELD ACCELERATOR *

R. Margraf-O'Neal[1†], A. Ody[1], J. Power[1], J. Hlavenka[1], B. N. Temizel Ozdemir[1,2], G. Andonian[3], B. Carlsten[4], A. DeSimone[1,2], G. Ha[1,2], A. Halavanau[5], H. Xu[4], N. Majernik[5], J. M. Maxson[6], A. Parrack[3], R. Ryne[7], M. Yadav[3,8], N. Yampolsky[4], J. Rosenzweig[3]
[1] Argonne National Laboratory, Lemont, IL, USA
[2] Northern Illinois University, DeKalb, IL, USA
[3] University of California - Los Angeles, Los Angeles, CA, USA
[4] Los Alamos National Laboratory, Los Alamos, NM, USA
[5] SLAC National Accelerator Laboratory, Menlo Park, CA, USA
[6] Cornell University, Ithaca, NY, USA
[7] Lawrence Berkeley National Laboratory, Berkeley, CA, USA
[8] Old Dominion University, Norfolk, VA, USA

*Abstract*

The emittance exchange (EEX) beamline at the Argonne Wakefield Accelerator (AWA) is designed to transfer properties of an electron beam phase space between the transverse and longitudinal planes. Recently, it has been proposed this beamline could be used to convert a microscale transverse modulation created by a TEM grid into a microbunch train in the longitudinal plane. Such a technique would be useful for obtaining nano-scale microbunching that does not rely on the sensitive process of FEL gain. This new approach has been proposed to enable development of a compact free-electron laser at Arizona State, greatly reducing size and cost compared with existing short wavelength FELs. To perform an exploratory demonstration of this concept at AWA, this experiment requires low normalized emittance ($\approx$50 nm $\cdot$ rad), low charge ($\approx$1 pC) electron bunches, and transverse diagnostics with high-resolution (1 - 3 µm) and high-light-collection to resolve the modulation on the electron beam. This report will give a progress update on preparing the necessary beams and diagnostics at AWA for an emittance exchange experiment that would produce 100s of nm scale microbunches.

## INTRODUCTION

X-Ray free-electron lasers (XFELs) rely on microbunching to produce exponential gain of short-wavelength X-ray radiation. This is most commonly done using a self-amplified spontaneous emission (SASE) process [1–6], where microbunches originate from noise, requiring a long undulator to build up microbunches. There are also many schemes that have been developed and implemented for seeded XFELs [7–10] and proposals for cavity-based XFELs [11, 12]. A recent proposal at Arizona State University [13, 14] described a method of FEL seeding by transforming transverse beamlets into longitudinal microbunches. This technique promises a highly efficient and compact method for generating microbunches, but is very sensitive to beam emittance, and collective effects such as space charge. Thus, the nanopatterned microbunching collaboration has been formed to perform a proof-of-principle experiment of this mechanism at the Argonne Wakefield Accelerator (AWA).

As depicted in Fig. 1, the nanopatterned microbunching experiment will produce beamlets by scattering on a 12.5 µm period grating. These will be demagnified using a quadrupole lattice to 3 µm, then transformed into 800 nm microbunches via an emittance exchange lattice. While 800 nm is too long of a wavelength to yet be useful for XFELs, this experiment will provide a proof of principle achievable within the constraints of the AWA facility that will be extendable to shorter wavelengths with higher energy beams where space charge effects are less dominant.

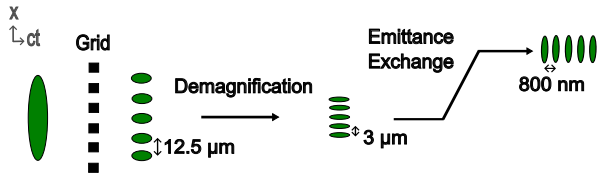


Figure 1: Overview of the nanopatterned microbunching experiment. Beamlets are created in the transverse plane using a TEM grid, demagnified to a 3 µm period using a quadrupole lattice, then transformed into longitudinal microbunches at 800 nm with an emittance exchange beamline.

The nanopatterned microbunching experiment has several requirements on the AWA facility that are outside of its normal operating range. AWA is tuneable within a large charge range (1 pC - 400 nC), but optimized for high charge (100s of nC) bunch trains to drive structure wakefield acceleration [15, 16]. However, to mitigate collective effects, the nanopatterned microbunching experiment must operate at

* This work is supported by the U. S. Department of Energy, under contract No. DE-AC02-06CH11357.
† rmargrafoneal@anl.gov

ISBN: 978-3-95450-261-5 ISSN: 2673-7000 doi: 10.18429/JACoW-NAPAC2025-MOP055



low charge (1 pC). Additionally, low normalized emittance (50 nm · rad) must be achieved to preserve the closely spaced transverse beamlets.

Finally, this experiment requires high-light collection, high-resolution (1 - 3 µm) transverse diagnostics, and longitudinal diagnostics sensitive to 800 nm microbunches. Longitudinal microbunches can be characterized using AWA's transverse deflecting cavities, and with coherent transition radiation (CTR) and undulator radiation methods that will be addressed in future work. This work will focus on low-charge, low emittance, and high transverse spatial resolution measurements.

## MEASUREMENTS

### *Charge*

AWA's primary charge detector is an integrated current transformer (ICT), which is sensitive down to 20 pC. AWA also has a beam position monitor (BPM). Summing the signal from the four channels of the BPM provides a more sensitive charge diagnostic. An example waveform is shown in Fig. 2A. When calibrated against the ICT signal, as shown in Fig. 2B, the BPM can detect charges down to ≈1 pC.

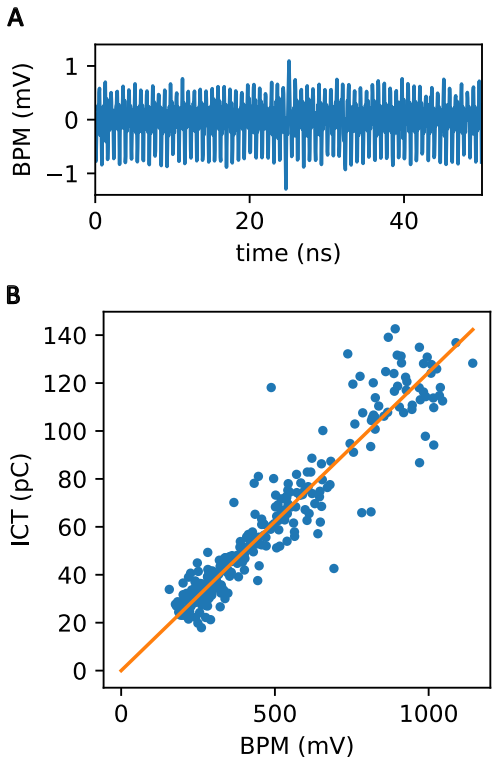


Figure 2: Low charge detection with a BPM. A) Time-dependent trace for a 0.8 pC bunch, showing a signal peak. B) Calibration of the BPM peak height against AWA's integrated current transformer (ICT).

For YAG screens (100 µm thick), we also contend with dark current. With non-gated cameras and nominal gun gradient, we can detect 0.4 pC/mm$^2$ before the beam approaches the dark current level, as shown in Fig. 3.

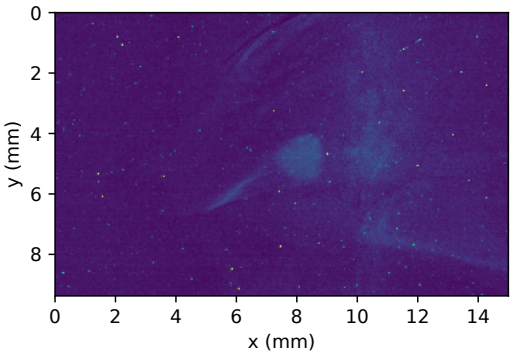


Figure 3: A 0.8 pC bunch expanded to ≈2.0 mm$^2$ (or $\sigma_x$ = 460 µm, $\sigma_y$ = 524 µm for a Gaussian fit). Background subtraction has been performed relative to the case with the photocathode laser off. At this level (0.4 pC/mm$^2$), the signal (solid spot in the center of the screen) is just above the dark current features (streaks and hazy charge distributions).

### *High-Resolution Transverse Diagnostics*

We installed a Blackfly camera (BFLY-PGE-23S6M-C) with a Nikon AF FX 200 mm f/4D IF-ED Lens and 357 mm extension tube. This was focused on a 100 µm thick YAG screen after a 45° mirror reflection. The light path distance from the YAG to the vacuum chamber window was 165 mm, and the working distance from the end of the camera lens to the YAG was 178 mm.

This set-up resulted in a 1.30 µm pixel size, a magnification factor of 4.5. The camera resolution was tested with a US Air Force target. On the bench top, the minimum resolvable feature size was 2.76 µm. With the vacuum window and mirror reflection, in the installed system the resolution was 4.92 µm.

Using this imaging system, we focused a ≈1 pC electron beam to a small spot. We first created a low-emittance electron beam using a FWHM=20 µm aperture in the homogenization plane of our laser, which is designed to make a FWHM=36 µm laser pulse on the photocathode after magnification. After acceleration to 40 MeV and quadrupole focusing, this created a $\sigma_x$ = 69 µm, $\sigma_y$ = 56 µm electron beam as shown in Fig. 4A. Repeating this measurement with a larger, FWHM=50 µm aperture, for a spot size on the photocathode of 90 µm, produced a $\sigma_x$ = 81 µm, $\sigma_y$ = 62 µm electron beam after focusing.

### *Quadrupole Scan Emittance Measurements*

Using the imaging system described in the previous section, we took quadrupole scans to measure emittance at ≈2 pC as shown in Fig. 5. A quadrupole 37.75 cm before the YAG screen was scanned for simultaneous measurement of the emittance in both X and Y. For Fig. 5A (20 µm aperture) normalized x emittance is 3.6 µm · rad. For Fig. 5B (50 µm aperture), normalized x emittance are 3.1 µm · rad and normalized y emittance is 3.7 µm · rad. These are larger than our 50 nm · rad emittance target.

ISBN: 978-3-95450-261-5 ISSN: 2673-7000 doi: 10.18429/JACoW-NAPAC2025-MOP055

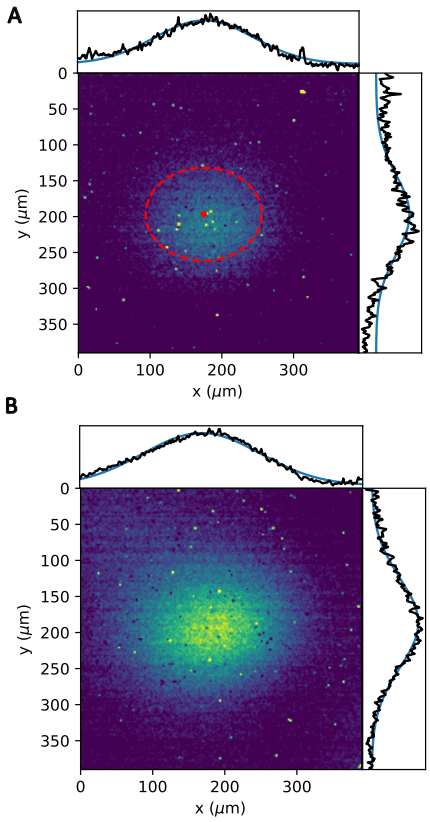


Figure 4: Focusing a ≈1 pC beam on a YAG. A) Beam generated from 36 µm laser spot on photocathode, B) Beam generated from 90 µm laser spot on photocathode. The RMS sizes of the beams are $\sigma_x = 69$ µm, $\sigma_y = 56$ µm, and $\sigma_x = 81$ µm, $\sigma_y = 62$ µm respectively.

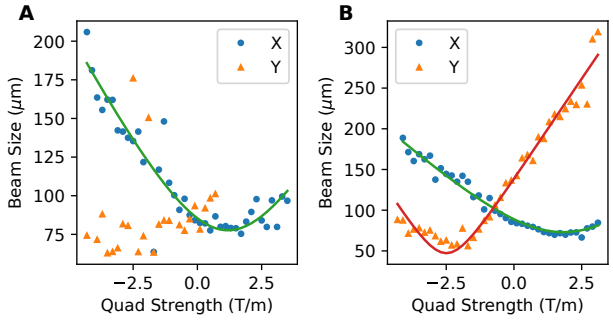


Figure 5: Quad scan emittance measurements at ≈2 pC. A) (20 µm aperture) $\epsilon_{x,N} = 3.6$ µm · rad. B) (50 µm aperture), $\epsilon_{x,N} = 3.1$ µm · rad and $\epsilon_{y,N} = 3.7$ µm · rad.

## DISCUSSION

We were surprised that we could not focus the beam to less than $\sigma = 60$ µm. If we were achieving our target $\epsilon_{x,N} = 50$ nm · rad, we would expect to be able to focus to the sub 10 µm level. The measurement of a larger beam might mean that we are resolution limited on the YAG screen, with the YAG blurring a smaller beam to appear as a larger beam. If this is the case, then the emittance measurement may also be incorrect, as the beam size may be overestimated by this measurement.

Alternatively, if the emittance measurement is as large as measured by our quadrupole scan, then this may be the smallest with which we can focus this electron beam. Further tests are needed to understand this measurement.

## FUTURE WORK

In the near term, we will repeat these quadrupole scan emittance measurements with a longer drift to bring the beam to a more gentle focus, within the minimum beam size measurable on the YAG. We will also perform alternative emittance measurement techniques, including a knife-edge scan.

We will also continue to optimize the AWA beamline for low emittance while maintaining reasonably low dark current. A high electron gun gradient helps preserve a low emittance, while increasing the dark current. We will find the optimal gradient that balances these two effects. We will also scan the strength of solenoids near the electron gun to characterize their effect on the emittance growth.

Prior to the nanopatterned microbunching experiment, we also plan to install thinner 20 µm thick YAG screens, and reduce the camera resolution to 1 µm to improve the quality of the transverse imaging system. Additionally, once we have the 12.5 µm transverse grid installed, we can characterize the emittance of the beamlets produced by the grid. Finally, we will address the longitudinal diagnostics needed by this experiment, both testing AWA's transverse deflecting cavity longitudinal characterization system at 1 pC, and considering the installation of CTR and undulator radiation production devices.

The AWA beamline still has a lot of preparation needed before achieving the low-charge, low-emittance condition with high-resolution diagnostics needed for the nanopatterned microbunching experiment. However, the results shown in this proceedings give us a clear picture of the necessary improvements needed that we will implement prior to the experiment.

## REFERENCES

[1] P. Emma *et al.*, "First lasing and operation of an ångstrom-wavelength free-electron laser", *Nat. Photonics*, vol. 4, no. 9, pp. 641–647, 2010. doi:10.1038/nphoton.2010.176

[2] T. Ishikawa *et al.*, "A compact X-ray free-electron laser emitting in the sub-ångström region", *Nat. Photonics*, vol. 6, no. 8, pp. 540–544, 2012. doi:10.1038/nphoton.2012.141

[3] H.-S. Kang *et al.*, "Hard X-ray free-electron laser with femtosecond-scale timing jitter", *Nat. Photonics*, vol. 11, no. 11, pp. 708–713, 2017. doi:10.1038/s41566-017-0029-8

[4] W. Decking *et al.*, "A MHz-repetition-rate hard X-ray free-electron laser driven by a superconducting linear accelerator", *Nat. Photonics*, vol. 14, no. 6, pp. 391–397, 2020. doi:10.1038/s41566-020-0607-z

ISBN: 978-3-95450-261-5 ISSN: 2673-7000 doi: 10.18429/JACoW-NAPAC2025-MOP055



[5] E. Prat *et al.*, "A compact and cost-effective hard X-ray free-electron laser driven by a high-brightness and low-energy electron beam", *Nat. Photonics*, vol. 14, no. 12, pp. 748–754, 2020. doi:10.1038/s41566-020-00712-8

[6] B. Liu *et al.*, "The SXFEL Upgrade: From Test Facility to User Facility", *Applied Sciences*, vol. 12, no. 1, p. 176, 2022. doi:10.3390/app12010176

[7] L. Yu *et al.*, "High-gain harmonic-generation free-electron laser", *Science*, vol. 289, no. 5481, pp. 932–935, 2000. doi:10.1126/science.289.5481.932

[8] G. Stupakov, "Using the Beam-Echo Effect for Generation of Short-Wavelength Radiation", *Phys. Rev. Lett.*, vol. 102, no. 7, p. 074 801, 2009. doi:10.1103/PhysRevLett.102.074801

[9] O. Y. Gorobtsov *et al.*, "Seeded X-ray free-electron laser generating radiation with laser statistical properties", *Nat. Commun.*, vol. 9, no. 1, p. 4498, 2018. doi:10.1038/s41467-018-06743-8

[10] I. Nam *et al.*, "High-brightness self-seeded X-ray free-electron laser covering the 3.5 keV to 14.6 keV range", *Nat. Photonics*, vol. 15, no. 6, pp. 435–441, 2021. doi:10.1038/s41566-021-00777-z

[11] R. Margraf *et al.*, "Low-loss stable storage of 1.2 Å X-ray pulses in a 14 m Bragg cavity", *Nat. Photonics*, vol. 17, no. 10, pp. 878–882, 2023. doi:10.1038/s41566-023-01267-0

[12] M. Singleton, J. Rosenzweig, J. Tang, and Z. Huang, "An Ultra-Compact X-ray Regenerative Amplifier Free-Electron Laser", *Instruments*, vol. 8, no. 1, 2024. doi:10.3390/instruments8010002

[13] W. Graves, "The CXFEL Project at Arizona State University", in *Proc. 67th ICFA Adv. Beam Dyn. Workshop Future Light Sources (FLS'23)*, Luzern, Switzerland, pp. 54–57, 2024. doi:10.18429/JACoW-FLS2023-TU1C4

[14] G. Ha *et al.*, "Coherent radiation from initially modulated beams using emittance exchange at the Argonne Wakefield Accelerator", *Nucl. Instrum. Methods Phys. Res., Sect. A*, vol. 1075, p. 170 387, 2025. doi:10.1016/j.nima.2025.170387

[15] L. Zheng *et al.*, "Rapid thermal emittance and quantum efficiency mapping of a cesium telluride cathode in an rf photoinjector using multiple laser beamlets", *Phys. Rev. Accel. Beams*, vol. 23, no. 5, p. 052 801, 2020. doi:10.1103/PhysRevAccelBeams.23.052801

[16] J. G. Power, M. E. Conde, W. Gai, Z. Li, and D. Mihalcea, "Upgrade of the Drive LINAC for the AWA Facility Dielectric Two-Beam Accelerator", pp. 4310–4312. http://accelconf.web.cern.ch/IPAC10/papers/THPD016.pdf